NMR characterization of sulphur substitution effects in the K_{x}Fe_{2−y}Se_{2−z}S_{z} high-T_{c} superconductor

D. A. Torchetti, T. Imai, H. C. Lei, and C. Petrovic

Phys. Rev. B **85**, 144516 — Published 17 April 2012

DOI: 10.1103/PhysRevB.85.144516

NMR Characterization of Sulphur Substitution Effects in the $K_xFe_{2-y}Se_{2-z}S_z$ high-T_c Superconductor

D. A. Torchetti[1], T. Imai[1,2], H. C. Lei [3], and C. Petrovic [3]
[1] *Department of Physics and Astronomy, McMaster University, Hamilton, Ontario, L8S 4M1, Canada*
[2] *Canadian Institute for Advanced Research, Toronto, Ontario, M5G 1Z8, Canada and*
[3] *Condensed Matter Physics and Materials Science Department, Brookhaven National Laboratory, Upton, New York, 11973, USA*
(Dated: February 22, 2012)

We present a ^{77}Se NMR study of the effect of S substitution in the high T_c superconductor, $K_xFe_{2-y}Se_{2-z}S_z$, in a temperature range up to 250 K. We examine two S concentrations, with z = 0.8 ($T_c \sim 26$ K) and z = 1.6 (non-superconducting). The samples containing sulphur exhibit broader NMR lineshapes than the $K_xFe_2Se_2$ sample due to local disorder in the Se environment. Our Knight shift ^{77}K data indicate that in all samples uniform spin susceptibility decreases with temperature, and that the magnitude of the Knight shift itself decreases with increased S concentration. In addition, S substitution progressively suppresses low frequency spin fluctuations. None of the samples exhibit an enhancement of low frequency antiferromagnetic spin fluctuations (AFSF) near T_c in $1/T_1T$, as seen in FeSe.

I. INTRODUCTION

With the discovery of high T_c superconductivity in the iron-arsenides in 2008,[1] researchers found renewed interest and hope in understanding the mechanism of high T_c superconductivity.[2–5] Although much has been learned, the superconducting mechanism is still poorly understood. Earlier reports suggest that optimal doping for superconductors places the system in the vicinity of magnetic instability as evidenced by the largest enhancement of antiferromagnetic spin fluctuations (AFSF) near T_c.[6–9] Fermi surface nesting between hole bands at the Brillouin zone center and electron bands near the zone edge may be associated with the AFSF, which in turn may cause Cooper pairing. In such a scenario, overdoping electrons suppresses the nesting effects by filling up the hole bands, and thereby suppressing AFSF and T_c.[8,9] In the simple iron-selenide superconductor, FeSe ($T_c \sim 9$ K[10–12]), application of pressure alone can also push T_c as high as 37 K.[13–15] Furthermore, AFSF were shown to enhance in direct correlation with the enhancement of pressure and T_c,[16] reinforcing the view that AFSF and the superconducting mechanism may be linked.

Recently, Guo *et al.* reported the discovery of superconductivity in $K_xFe_{2-y}Se_2$.[17] Through intercalation of K into FeSe, T_c is again pushed much higher ($\sim$ 33 K). Recent ARPES measurements, however, revealed that unlike in iron-arsenide high T_c systems, *all* the hole bands near the center of the first Brillouin zone may be filled by electrons donated by K^+ ions.[18] This means that Fermi surface nesting effects would not induce AFSF, yet T_c is still very high. In fact, Earlier NMR results revealed no enhancement of the AFSF toward T_c in this system.[19–21]

In the present study, we explore the effect of substituting sulphur (S) into the Se sites of $K_xFe_{2-y}Se_{2-z}S_z$.[22,23] As shown in the phase diagram in Fig. 1, S substitution progressively suppresses T_c, enabling us to conduct a systematic microscopic NMR investigation of the evolution of electronic properties in going from a high-T_c superconductor to a non-superconductor. We examine two concentrations, one with z = 0.8 (40% substitution), and one with z = 1.6 (80% substitution), and compare the new NMR results with our report for $K_xFe_{2-y}Se_2$ (z = 0).[21] Sulphur substitution tends to generate a chemical pressure in the system, because S and Se have the same valence but S has an ionic radius less than half of that of Se. The lattice constant along the crystal *c*-axis indeed decreases from $\sim$14.0 to 13.9 Å and then to 13.7 Å as S concentration goes from z = 0 to 0.8 to 1.6, respectively; the lattice is compressed within the *ab* plane as well, so overall the Fe-Se bond length is shortened.[23] The systematic suppression of T_c with S substitution mimics the situation in FeSe, where over-pressurizing results in suppression of T_c.[13] The evolution of electronic properties in overpressured FeSe has been poorly explored because extremely high pressure ($\geq$ 9 GPa) is required.[13] Thus a microscopic investigation of S-substituted $K_xFe_{2-y}Se_2$ may provide us with a new path to investigate the possible correlations between T_c, structure, and AFSF when physical or chemical pressure suppresses T_c.

In what follows we will present new ^{77}Se NMR data for $K_xFe_{2-y}Se_{2-z}S_z$, and show that spin excitations are suppressed with S substitution. In section II we will briefly present our experimental procedures. In section III we will summarize our experimental results, paying particular attention to NMR Knight shift and nuclear spin-lattice relaxation rate $1/T_1$ data, and discuss some implications. In section IV we summarize our findings and conclude.

II. EXPERIMENTAL

Single crystals of $K_xFe_{2-y}Se_{2-z}S_z$ were grown using the self-flux method. Powder X-ray diffraction (XRD) measurements were obtained at 300 K using 0.3184 Å wave-length radiation on ground samples. The XRD data were then refined with the General Struc-

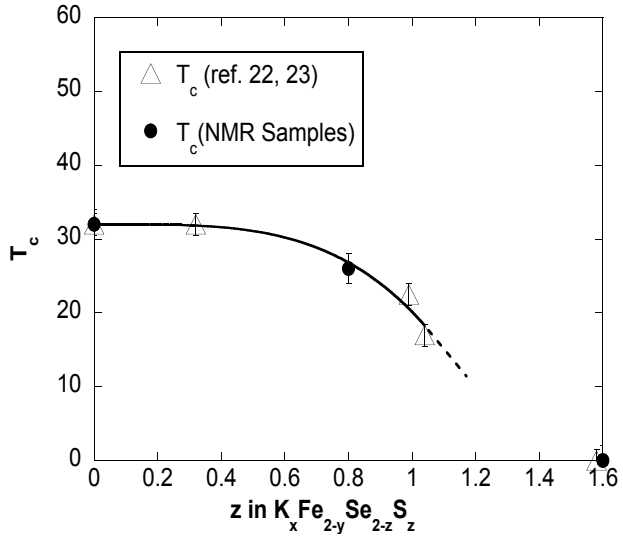

FIG. 1. (Color Online) Superconducting transition temperature, T_c, as a function of sulphur concentration, z. Filled circles represent current samples used for NMR, measured *in situ* in zero magnetic field, while open triangles represent data at the source of crystal growth.[22] Solid and dashed lines are a 'guide-to-eye'.

ture Analysis System.[24,25] Average stoichiometries were determined using energy-dispersive X-ray spectroscopy (EDX) in a JEOL JSM-6500 scanning electron microscope. The XRD data show superlattice reflections which incorporate an Fe ordered vacancy site. Potassium content as well as Fe defect content increase slightly with S substitution, as $x \sim 0.64$, 0.7, and 0.8 in $K_xFe_{2-y}Se_2$, $K_xFe_{2-y}Se_{1.2}S_{0.8}$, and $K_xFe_{2-y}Se_{0.4}S_{1.6}$ respectively. Full detail of the growth method, structural refinement, phase diagram, and other properties may be found elsewhere.[22,23,26,27] We determined the T_c of each of our NMR samples *in situ* by measuring the frequency shift of our NMR tank circuit.[21] The T_c of our NMR samples is summarized in Fig. 1, together with other compositions.

We carried out NMR measurements in an applied magnetic field of B = 8.33 Tesla applied along the crystal *c*-axis. By taking the Fast Fourier Transformation (FFT) of the envelope of the spin-echo we were able to obtain our NMR lineshapes. To measure the nuclear spin-lattice relaxation rate, $1/T_1$, we applied an inversion π pulse or saturation comb pulses prior to our spin-echo sequence.

III. RESULTS AND DISCUSSION

A. Uniform Spin Susceptibility

In Fig. 2 we compare ^{77}Se NMR lineshapes for different sulphur concentrations. Once scaled according to Selenium content in each crystal, integrated intensities for each system are equal within experimental uncertainties. The narrowest lineshapes are observed for the $z = 0$ sample; both S substituted samples exhibit line broadening, indicative of disorder effects in local electronic and structural properties at the Se sites.

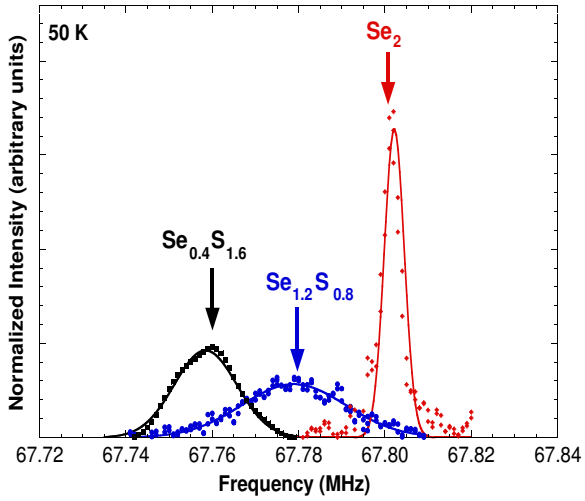

FIG. 2. (Color Online) Representative ^{77}Se NMR FFT lineshapes of $K_xFe_{2-y}Se_{2-z}S_z$ for z = 0.8 and z = 1.6 at 50 K, observed in B = 8.33 T. We also show $K_xFe_{2-y}Se_2$ for comparison.[21] The lineshapes have been normalized for an equal integrated intensity and fitted with Gaussian curves with Full Widths at Half Maximum (FWHM) $\sim$ 4.5 KHz, 24 KHz, and 14 KHz for z = 0, 0.8, and 1.6, respectively. Note the systematic lowering of the NMR peak frequency with increased S content.

In addition to the change in shape of the FFT, the NMR peak frequency is systematically lowered with increasing z. Peaks for the z = 0.8 and z = 1.6 samples are found at 67.78 MHz and 67.76 MHz respectively. With an expected Larmor frequency of $f_0 = \gamma_n$ B = 67.622 MHz, where $\gamma_n/2\pi = 8.118$ MHz/T is the *gyromagnetic ratio* for ^{77}Se, this means that the *Knight Shift* is lowered with increasing S concentration as well.

The ^{77}Se NMR Knight shift, ^{77}K, may be written as

$$^{77}K = \frac{A_{hf}}{g\mu_B}\chi_{spin} + K_{chem}. \quad (1)$$

A_{hf} is the hyperfine coupling constant between the ^{77}Se nuclear spins which we are observing and electron spins in their vicinity. χ_{spin} is the average spin susceptibility of these electrons. The Knight shift is therefore an excellent probe for the uniform $\mathbf{q = 0}$ wave vector mode of local spin susceptibility in bulk materials, free from the influence of impurity phases. K_{chem} is a temperature independent chemical shift which arises from the orbital motion of electrons. From the measurements below T_c in $K_xFe_2Se_2$ we estimate the lower bound of K_{chem} to be ~ 0.11 % without diamagnetic corrections.[21] K_{chem} may be slightly dependent on S-substitution effects.

In Fig. 3 we summarize the temperature and S-content dependence of ^{77}K. We find some qualitative similarities in the behaviour of all three compositions, but the magnitude of the spin contribution to the shift is reduced significantly in the S substituted samples near room temperature. In principle, the overall suppression of the spin contribution $^{77}K_{spin} = \frac{A_{hf}}{g\mu_B}\chi_{spin}$ may be caused by a reduction in the hyperfine coupling constant, A_{hf}, induced by structural changes. However, the Fe-Se bond length shortens as one substitutes S,[23] which would cause greater overlap of wavefunctions between Fe and Se(S) layers. Naively, A_{hf} would therefore become larger. Since we see an overall *decrease* in Knight shift, this implies χ_{spin} would have to drop more substantially if A_{hf} indeed increases. That is, our results in Fig. 3 imply that S substitution suppresses χ_{spin}.

Turning our attention to the temperature dependence of ^{77}K, all samples exhibit a monotonic decrease in Knight shift with temperature, which is consistent with behaviour previously reported in other iron-based superconductors such as $LaFeAsO_{1-x}F_x$,[6,28] $Ba(Fe_{1-x}Co_x)_2As_2$,[7–9,29], FeSe,[16], and $Ba_xK_{1-x}Fe_2As_2$.[30] In $Ba(Fe_{1-x}Co_x)_2As_2$ the temperature dependence of Knight shift remains qualitatively similar regardless of doping level.[8,9] In the present case, however, the temperature dependence becomes far less pronounced with S substitution. The increase in Knight shift at higher temperature for the undoped (z = 0) sample may be caused by the presence of excited states of the spins, which may be reached at higher temperatures with sufficient thermal energy. In such a pseudo-gap scenario,[6,28] our new observation implies that in the S-substituted systems either these excited states are diminished or the energy threshold required to excite spins is too great (and beyond our temperature range).

The dashed line through each of the three samples represents a purely phenomenological fit to the normal state data, with $^{77}K \sim \alpha + \beta \exp(-\Delta/k_BT)$, where Δ represents a pseudo-gap, α represents the ^{77}K value near T_c, and β is a constant. We had hoped to find a systematic change in Δ with S substitution but the uncertainty in its magnitude is too large because it is extremely sensitive to the choice of α. In fact, *all three* samples can be fit with the same $\Delta/k_B = 435$ K as previously found for undoped $K_xFe_{2-y}Se_2$.[21] We emphasize that Δ can be varied by as much as a factor of 2 while still maintaining a good fit to the data, and so it does not provide sufficient resolution to discern the difference between the pseudo-gaps. We have previously encountered this situation in $Ba(Fe_{1-x}Co_x)_2As_2$.[8]

Within a conventional Fermi liquid picture, the Knight shift would be dominated by Pauli spin susceptibility, $\chi_{spin} = \mu_B^2 N(E_F)$. A decrease in ^{77}K therefore might suggest that the density of states at the Fermi energy, $N(E_F)$, decreases as the concentration of S increases and temperature decreases. To check such a scenario beyond the $\mathbf{q} = \mathbf{0}$ mode of spin susceptibility, we must examine the nuclear spin-lattice relaxation rate, $1/T_1$.

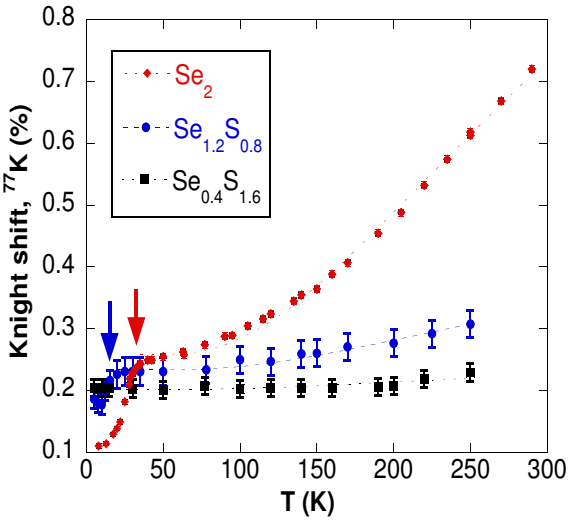

FIG. 3. (Color Online) Temperature dependence of the ^{77}Se NMR Knight shift, ^{77}K, along the *c*-axis. $K_xFe_{2-y}Se_2$ is presented for comparison. Arrows mark $T_c = 25$ K (z = 0) and 13 K (z = 0.8) in B = 8.33 T for the two superconducting samples as determined *in situ* by the change in tuning frequency of the NMR tank circuit. The dashed curve is a phenomenological fit with a pseudo-gap, $^{77}K \sim \alpha + \beta \exp(-\Delta/k_BT)$, with $\Delta/k_B = 435$ K for all samples. Overall, ^{77}K and therefore the $\mathbf{q} = \mathbf{0}$ component of χ_{spin} are suppressed with increased S doping.

B. Low Frequency Spin Fluctuations

Fig. 4 shows representative signal recovery after saturation recorded for T_1 measurements for all three samples. Single exponential fits are satisfactory for all compositions, as expected for ^{77}Se with nuclear spin I = 1/2. We can clearly see the general trend that substitution of S slows the spin-lattice relaxation. In Fig. 5 we present $1/T_1T$ (i.e. $1/T_1$ divided by T) as a function of temperature. $1/T_1T$ measures the wave-vector $\mathbf{q}$ integral of the imaginary part of the dynamical spin susceptibility, $\chi''(\mathbf{q}, f_{NMR})$, in the first Brillouin zone;

$$1/T_1T \propto \Sigma_q |A_{hf}(\mathbf{q})|^2 \frac{\chi''(\mathbf{q}, f_{NMR})}{f_{NMR}}, \qquad (2)$$

where $A_{hf}(\mathbf{q})$ is the wave vector dependent hyperfine form factor, and $f_{NMR} \sim 67.78$ MHz is the resonance frequency. In the optimally doped regime, many iron-arsenide systems show an enhancement of low frequency AFSF as reflected by $1/T_1T$ as one approaches T_c with decreasing temperature.[6–9,30] The FeSe system exhibits an analogous enhancement of AFSF as well, and a greater enhancement in AFSF reflected by $1/T_1T$ correlates with higher T_c.[16] For $Ba(Fe_{1-x}Co_x)_2As_2$, once the system enters the overdoped regime the enhancement of AFSF and T_c both begin to decrease.[8]

In $K_xFe_{2-y}Se_2$, $1/T_1T$ decreases sharply with temper-

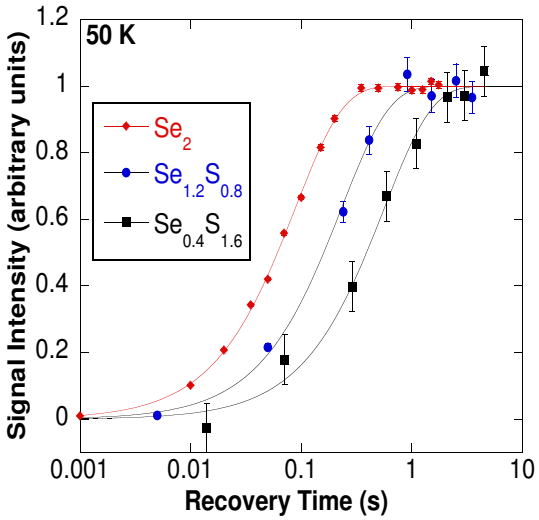

FIG. 4. (Color Online) Representative T_1 recovery curves measured at the center of the FFT lineshapes in Fig. 1 at 50 K. We normalize signal intensity for clarity. Solid lines represent single exponential fits through each data set, the argument of which gives our T_1 value. The strong trend toward slower relaxation rate with increased S substitution is evident.

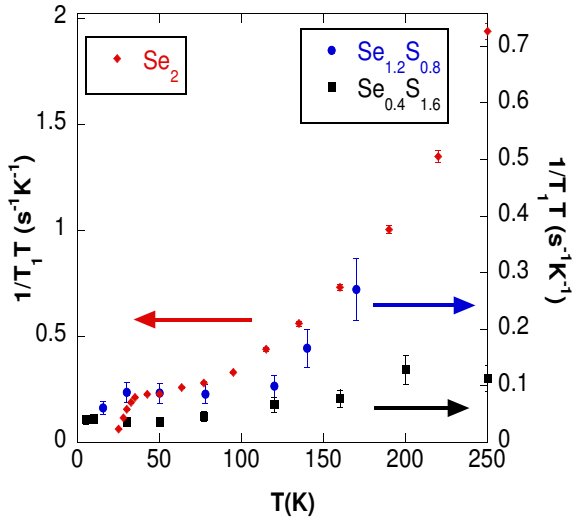

FIG. 5. (Color Online) $1/T_1T$ as a function of temperature for z = 0, 0.8, and 1.6, with magnetic field B = 8.33 T applied along the crystal *c*-axis. Relaxation rate gets progressively slower with S substitution; temperature dependence weakens as well. Neither of the two superconducting samples exhibit an enhancement toward T_c, and S substituted samples show nearly flat behaviour except for near room temperature.

ature below 300 K, then levels off toward T_c.[19–21] The lack of enhancement in $1/T_1T$ near T_c is analogous to the case of overdoped $Ba(Fe_{1-x}Co_x)_2As_2$ and suggests that $K_xFe_{2-y}Se_2$ may already be in the overdoped regime. In $K_xFe_{2-y}Se_{1.2}S_{0.8}$ we observed an analogous trend with overall suppression of $1/T_1T$, and hence spin excitations. Thus suppression of T_c with S substitution in Fig. 1 is accompanied by suppresion of spin excitations. For non-superconducting $K_xFe_{2-y}Se_{0.4}S_{1.6}$, $1/T_1T$ is nearly temperature independent, similar to overdoped, non-superconducting, metallic $Ba(Fe_{0.7}Co_{0.3})_2As_2$.[8] We caution that our finding does not necessarily imply there are no antiferromagnetic correlations in these systems. Our results in Fig. 5 do not rule out the possible enhancement of AFSF at energy scales much higher than $\hbar f_{NMR} \sim \mu$eV. In addition, $1/T_1T$ measures the *summation* of the wave-vector **q**, Σ_q, meaning that small AFSF may be present for some **q**-modes, and only that the net sum shows no enhancement.

In Fig. 6 we plot $1/\sqrt{T_1T}$ vs $^{77}K(\%)$. In a canonical Fermi liquid, $1/T_1T \propto N(E_F)^2$ as a result of Fermi's golden rule. The Korringa relation,

$$1/\sqrt{T_1T} = C\,(^{77}K_{spin}) + K_{chem}, \qquad (3)$$

where C is a constant and $^{77}K_{spin} \equiv \frac{A_{hf}}{g\mu_B}\chi_{spin}$ represents the spin contribution to Knight shift, is thus an excellent test for the applicability of Fermi liquid theory in this system. The undoped sample exhibits negative curvature in Fig. 6, and as reported earlier it does not appear to fit the Korringa relation.[20,21] $K_xFe_{2-y}Se_{1.2}S_{0.8}$ also exhibits positive curvature, which suggests that it does not fit in a simple Fermi liquid picture either. The $K_xFe_{2-y}Se_{0.4}S_{1.6}$ data may exhibit a somewhat closer to linear relationship, but this could be fictitious in view of the very weak temperature dependences of ^{77}K and $1/T_1T$ in the temperature range of our investigation. In addition, extrapolation of the apparent linear fit to the intercept of the horizontal axis implies K_{chem} is as large as $\sim 0.22\%$ for $K_xFe_{2-y}Se_{0.4}S_{1.6}$. That is, if the Fermi liquid picture applies to the non-superconducting $K_xFe_{2-y}Se_{0.4}S_{1.6}$, K_{chem} would have to double in magnitude compared with superconducting $K_xFe_{2-y}S_2$.

IV. SUMMARY

In this paper we have reported a systematic variation of the electronic properties of the recently discovered high T_c superconductor, $K_xFe_{2-y}Se_{2-z}S_z$ with z = 0, 0.8, and 1.6, where S substitution generates chemical pressure. Using ^{77}Se NMR, we have taken measurements of Knight shift, ^{77}K, and nuclear spin-lattice relaxation rate, $1/T_1$, in a temperature range of up to 250 K. The NMR results observed for the superconducting z = 0.8 sample ($T_c \sim 26$ K) are analogous to those observed for the z = 0 sample ($T_c \sim 33$ K) and overdoped $Ba(Fe_{1-x}Co_x)_2As_2$. Specifically, the pseudogap-like behaviour with growing ^{77}K and $1/T_1T$ at higher temperatures is strongly suppressed by S substitution. The pseudogap-like behaviour is nearly non-existent for the non-superconducting z = 1.6 sample.

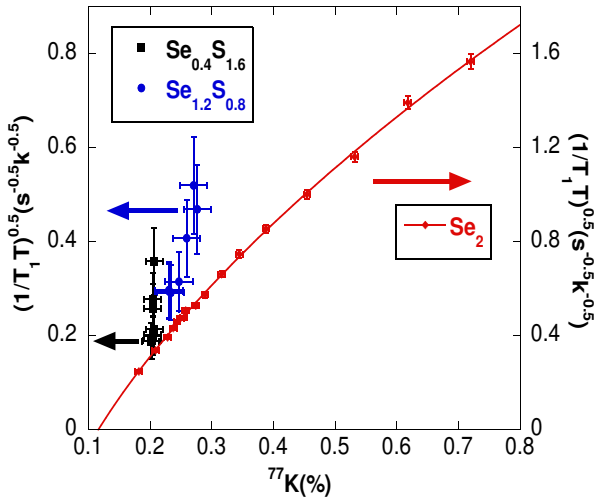

FIG. 6. (Colour Online) $1/\sqrt{T_1T}$ vs $^{77}K(\%)$. A constant slope would indicate the presence of the Korringa relation, an indicator for Fermi liquid theory. The extrapolated horizontal intercept corresponds to K_{chem}. The solid line through the undoped sample is a free parameter fit for $1/\mathrm{T_1T} = (^{77}K - K_{chem})^n$, where $n \sim 1.6$ instead of the Fermi liquid value of $n \sim 2$, with the horizontal intercept $K_{chem} \sim 0.11\%$.

None of the $K_xFe_{2-y}Se_{2-z}S_z$ systems *conclusively* satisfy the Korringa relation expected for canonical Fermi liquids, but the z = 1.6 composition may in fact be closer to a Fermi liquid.

It has been suggested that in Fe-As systems, the pnictogen height, i.e. the distance between the pnictogen and the Fe plane, acts as a tuner for superconductivity, where a certain height optimizes T_c.[31] In addition, in the $FeSe_{1-x}S_x$ system it was reported that T_c increased with S substitution up to 20%, then decreased with further substitution.[32] Given that S substitution only lowers T_c in our samples,[22,23] along with our results showing suppression of spin susceptibility and spin excitations similar to overdoped Fe-based systems, this suggests that increasing S content is analogous to *over-pressurizing* the system beyond the optimum Fe-Se height.

ACKNOWLEDGMENTS

Work at McMaster is supported by NSERC and CIFAR. Work at Brookhaven is supported by the U.S. DOE under Contract No. DE-AC02-98CH10886 and in part by the Center for Emergent Superconductivity, an Energy Frontier Research Center funded by the U.S. DOE, Office for Basic Energy Science (H.C.Lei and C.P).

[1] Y. Kamihara, T. Watanabe, M. Hirano, and H. Hosono, J. Amer. Chem. Soc. **130**, 3296 (2008).
[2] M. Norman, Physics **1**, 21 (2008).
[3] C. Day, Physics Today **62**, 36 (2009).
[4] J. Paglione and R. L. Greene, Nature Physics **6**, 645 (2010).
[5] D. C. Johnston, Advances in Physics **59**, 803 (2010).
[6] Y. Nakai, K. Ishida, Y. Kamihara, M. Hirano, and H. Hosono, J. Phys. Soc. Jpn. **77**, 073701 (2008).
[7] F. Ning, K. Ahilan, T. Imai, A. S. Sefat, R. Jin, M. A. McGuire, B. C. Sales, and D. Mandrus, J. Phys. Soc. Jpn. **77**, 103705 (2008).
[8] F. L. Ning, K. Ahilan, T. Imai, A. S. Sefat, M. A. McGuire, B. C. Sales, D. Mandrus, P. Cheng, B. Shen, and H.-H. Wen, Phys. Rev. Lett. **104**, 037001 (2010).
[9] F. Ning, K. Ahilan, T. Imai, A. S. Sefat, R. Jin, M. A. McGuire, B. C. Sales, and D. Mandrus, J. Phys. Soc. Jpn. **78**, 013711 (2009).
[10] F. C. Hsu, J. Y. Luo, K. W. Yeh, T. K. Chen, T. W. Huang, P. M. Wu, Y. C. Lee, Y. L. Huang, Y. Y. Chu, D. C. Yan, and M. K. Wu, Proc. Nat. Acad. Sci. **105**, 14262 (2008).
[11] T. M. McQueen, Q. Huang, V. Ksenofontov, C. Felser, Q. Xu, H. Zandbergen, Y. S. Hor, J. Allred, A. J. Williams, D. Qu, J. Checkelsky, N. P. Ong, and R. J. Cava, Phys. Rev. B. **79**, 014522 (2009).
[12] Y. Mizuguchi, F. Tomioka, S. Tsuda, T. Yamaguchi, and Y. Takano, Appl. Phys. Lett. **93**, 152505 (2008).
[13] S. Medvedev, T. M. McQueen, I. Trojan, T. Palasyuk, M. I. Erements, R. J. Cava, S. Naghavi, F. Casper, V. Ksenofontov, G. Wortmann, and C. Felser, Nature Materials **8**, 630 (2009).
[14] S. Margadonna, Y. Takabayashi, Y. Ohishi, Y. Mizuguchi, Y. Takano, T. Kagayama, T. Nakagawa, M. Takata, and K. Prassides, Phys. Rev. B. **80**, 064506 (2009).
[15] Y. Mizuguchi, , F. Tomioka, S. Tsuda, T. Yamaguchi, and Y. Takano, Physica C **470**, S353 (2010).
[16] T. Imai, K. Ahilan, F. L. Ning, T. M. McQueen, and R. J. Cava, Phys. Rev. Lett. **102**, 177005 (2009).
[17] J. Guo, S. Jin, G. Wang,S. Wang, K. Zhu, T. Zhou, M. He, and X. Chen, Phys. Rev. B. **82**, 180520 (2010).
[18] T. Qian, X.-P. Wang, W.-C. Jin, P. Zhang, P. Richard, G. Xu, X. Dai, Z. Fang, J.-G. Guo, X.-L. Chen, and H. Ding, Phys. Rev. Lett. **106**, 187001 (2011).
[19] W. Yu, L. Ma, J. B. He, D. M. Wang, T.-L. Xia, G. F. Chen, and W. Bao, Phys. Rev. Lett. **106**, 197001 (2011).
[20] H. Kotegawa, Y. Hara, H. Nohara, H. Tou, Y. Mizuguchi, H. Takeya, and Y. Takano, J. Phys. Soc. Jpn. **80**, 043708 (2011).
[21] D. A. Torchetti, M. Fu, D. C. Christensen, K. J. Nelson, T. Imai, H. C. Lei, and C. Petrovic, Phys. Rev. B. **83**, 104508 (2011).
[22] H. Lei, M. Abeykoon, E. S. Bozin, and C. Petrovic, Phys. Rev. B. **83**, 180503 (2011).
[23] H. Lei, M. Abeykoon, E. S. Bozin, K. Wang, J. B. Warren, and C. Petrovic, Phys. Rev. Lett. **107**, 137002 (2011).
[24] A. C. Larson and R. B. V. Dreele, Los Alamos National Laboratory Report LAUR , 86 (1994).
[25] B. H. Toby, J. Appl. Crystallogr. **34**, 210 (2001).
[26] H. Lei and C. Petrovic, Europhys. Lett. **95**, 57006 (2011).
[27] H. Lei and C. Petrovic, Phys. Rev. B. **84**, 052507 (2011).
[28] K. Ahilan, F. L. Ning, T. Imai, A. S. Sefat, R. Jin, M. A. McGuire, B. C. Sales, and D. Mandrus, Phys. Rev. B. **78**,

100501 (2008).
[29] X. F. Wang, T. Wu, G. Wu, H. Chen, Y. L. Xie, J. J. Ying, Y. J. Yan, R. H. Liu, and X. H. Chen, Phys. Rev. Lett. **102**, 117005 (2009).
[30] K. Matano, Z. Li, G. L. Sun, D. L. Sun, C. T. Lin, M. Ichioka, and G. Zheng, Europhys. Lett. **87**, 27012 (2009).
[31] K. Kuroki, H. Usui, S. Onari, R. Arita, and H. Aoki, Phys. Rev. B. **79**, 224511 (2009).
[32] Y. Mizuguchi, F. Tomioka, S. Tsuda, T. Yamaguchi, and Y. Takano, J. Phys. Soc. Jpn. **78**, 074712 (2009).

A. ^{77}Se NMR Characterization

In Fig. 1 we summarize the change of tuning frequency of the NMR circuit, Δf_{tune}(T) as a function of temperature. The tuning frequency is related to inductance via

$$f_{tune} \sim \frac{1}{\sqrt{LC}}, \tag{4}$$

where L and C are the inductance and capacitance of the circuit, respectively. When a system undergoes a superconducting phase transition, the bulk magnetic susceptibility, χ_{bulk}, suddenly becomes negative due to superconducting Meissner effects. The inductance, $L = L_0(1 + \eta\chi_{bulk})$, where η is a filling factor, will therefore decrease suddenly below T_c, causing an increase in tuning frequency easily observed by our network analyser.

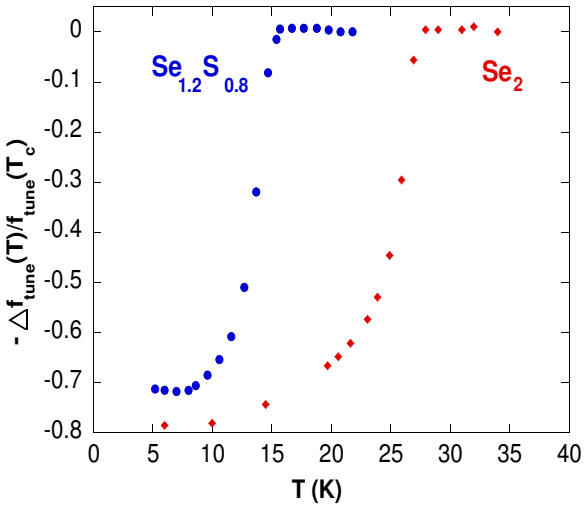

FIG. 7. (Color Online) The change in tuning frequency, -$\Delta f_{tune}(T)$ of our NMR circuit for B = 8.33 T. Meissner effects brought on during the superconducting transition change the inductance in our NMR coil. T_c is suppressed with S substitution.

We plot -$\Delta f_{tune}(T)$, normalized by dividing by $f_{tune}(T_c)$. The $K_xFe_{2-y}Se_{0.4}S_{1.6}$ system is precisely the concentration of S where superconductivity is destroyed.[23] $K_xFe_{2-y}Se_{1.2}S_{0.8}$ exhibits a superconducting phase transition, however, and we use the change in tuning frequency to determine where it takes place. We see that an onset as high as $T_c \sim 16$ K is observed, followed by a moderately sharp superconducting transition. Our earlier results for $K_xFe_{2-y}Se_2$ are presented as well for comparison.[21]